Journal of Biomedical Optics

SPIEDigitalLibrary.org/jbo

Dependence of light scattering profile in tissue on blood vessel diameter and distribution: a computer simulation study

Hamootal Duadi
Dror Fixler
Rachela Popovtzer

SPIE

Dependence of light scattering profile in tissue on blood vessel diameter and distribution: a computer simulation study

Hamootal Duadi, Dror Fixler, and Rachela Popovtzer
Bar-Ilan University, Institute of Nanotechnology and Advanced Materials, Faculty of Engineering, Ramat-Gan 52900, Israel

Abstract. Most methods for measuring light–tissue interactions focus on the volume reflectance while very few measure the transmission. We investigate both diffusion reflection and diffuse transmission at all exit angles to receive the full scattering profile. We also investigate the influence of blood vessel diameter on the scattering profile of a circular tissue. The photon propagation path at a wavelength of 850 nm is calculated from the absorption and scattering constants via Monte Carlo simulation. Several simulations are performed where a different vessel diameter and location were chosen but the blood volume was kept constant. The fraction of photons exiting the tissue at several central angles is presented for each vessel diameter. The main result is that there is a central angle that below which the photon transmission decreased for lower vessel diameters while above this angle the opposite occurred. We find this central angle to be 135 deg for a two-dimensional 10-mm diameter circular tissue cross-section containing blood vessels. These findings can be useful for monitoring blood perfusion and oxygen delivery in the ear lobe and pinched tissues. [DOI: 10.1117/1.JBO.18.11.111408]

Keywords: light–tissue interaction; diffusion reflection; diffuse transmission; Monte Carlo simulation.

Paper 130235SSRR received Apr. 11, 2013; revised manuscript received Jun. 19, 2013; accepted for publication Jun. 28, 2013; published online Jul. 25, 2013.

1 Introduction

Most optical-physiological diagnosis methods are based on the insertion of light, with known parameters to a tested tissue, followed by the measurement of the re-emitted light. When investigating light–tissue interactions, human tissue is usually dealt with as a semi-infinite surface. Hence, the light reflected from the tissue (volume reflection) is commonly investigated.[1–6] Very few methods test the transmitted light[7–10] or ballistic photons.[11] In this work, we suggest looking at the full profile of scattered light (transmitted and reflected) from a circle of tissue, such as a fingertip joint, ear lobe, or pinched tissue, at all possible exit angles. This full profile will reveal new behaviors of photon migration in tissue.

The human tissue is one of the most complex optical mediums since it is a turbid one, which means it is not homogeneous. Hence the optical properties, such as the absorption coefficient μ_a, the scattering coefficient μ_s, and the anisotropy factor g, are unknown and vary in different areas and physiological states. Furthermore, during respiration the blood vessels, which are the main cause for light absorption, vary in size.

Since the blood vessel distribution in the tissue is not homogenous, several researchers[12–15] raised the question whether the attenuation due to absorption in the blood also depends on the distribution of the blood vessels in the tissue. Liu et al.[10] used an epoxy phantom to demonstrate that the inner part of larger blood vessels is less effective in light absorption because it has lower exposure to light ("shielding effect"). By using computer simulation, Jacques[13] found that the reflectance from a semi-infinite tissue increases with a direct correlation to the vessel size, even though blood volume was kept constant.

Measurements of light–tissue interaction involve either direct methods which need no theoretical models of light propagation, or indirect methods. Direct methods include attenuation measurements in calibration solutions[16] or integrating spheres for the measurement of the total light transmission through a blood sample and of the total reflected light.[7–9]

Indirect methods are based on mathematical simulation models of photon migration. Photon migration simulations are commonly described by the diffusion theory.[17] However, in the close region near the light source, diffusion theory does not accurately describe the light distribution.[18] The Monte Carlo (MC) simulation method assumes that all photons begin as ballistic photons, and the change in their direction is due to the scattering coefficient of the medium.[1,11,13,19,20]

In this work, we calculated via MC simulation the distribution of collected photons after being scattered and absorbed in a two-dimensional (2-D) model of a circular cross section of tissue containing blood vessels. The results were compared to three-dimensional (3-D) where the transmission profile was calculated. A near infrared (NIR) wavelength of 850 nm was chosen due to its high penetration depth and minimal scattering.[21] The numerical simulation was repeated ten times to eliminate vessel location dependency. The transmission and reflectance profiles via blood vessel diameter was extracted from our results in order to compare them to traditional known results.

2 Materials and Methods

2.1 *Model of Tissue with Blood Vessels*

The 2-D 10-mm diameter circular cross section of "tissue" in which circles of "blood vessels" were introduced is shown in

Address all correspondence to: Dror Fixler, Bar-Ilan University, Institute of Nanotechnology and Advanced Materials, Faculty of Engineering, Ramat-Gan 52900, Israel. Tel: +972-3-5317598; Fax: +972-3-7384050; E-mail: Dror.Fixler@biu.ac.il

0091-3286/2013/$25.00 © 2013 SPIE

Fig. 1. To understand the influence of the vessel diameter, several simulations were held where a different vessel diameter was chosen. In order to fulfill the constant blood volume (denoted K) condition, the number of vessels n having a diameter D was chosen using

$$K = n\pi(D/2)^2, \tag{1}$$

so the total volume of the blood is constant for all blood vessel diameter groups.

The location of these n vessels was chosen randomly while verifying that there are no overlaps.

A 3-D model of a cylinder of tissue with absorbent blood vessels randomly placed in the xz plane and uniform in the y direction were created with the same method and properties as described in the 2-D model (Fig. 2). Ten repetitions of the simulation, where the number of vessels and their diameter was the same but their location was changed, were held to determine the variations in transmission due to the random vessel location. The illumination was set to be a square of 1.5× 1.5 mm^2, and the transmitted photons were collected from a 1 mm thick slice (gray area in Fig. 2) along the cylinder surface. Although the cylindrical geometry description is well known in the literature,[22] to the best of our knowledge this is the first time its full scattering profile for 360 deg over the sample has been simulated.

2.2 *Numerical MC Simulation of Photon Migration*

A beam of photons with a waist of $w_0 = 1.5$ mm enters the circular tissue parallel to the z direction. Note that due to the diffraction theory limitations, the distinction between different blood vessel diameters in the scattering profile is only valid when illuminating with a beam waist several orders of magnitude higher than the vessel diameters. In the NIR wavelength of 850 nm chosen in this work, the vessels act as absorbing and

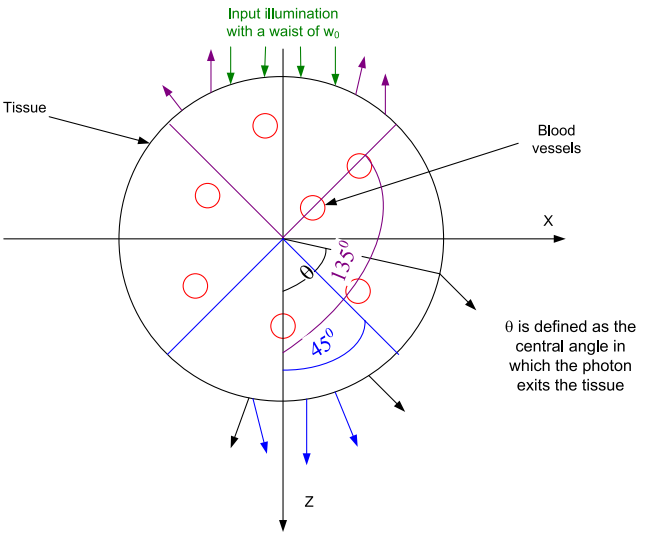

Fig. 1 Scheme of simulated 2-D model. Blood vessels (small red circles) were randomly placed in a homogenic tissue (black circle). A beam of photons with a waist of w_0 was introduced at one end (green arrows) in a direction of 0 deg central angle and collected at all central angles. Reflected photons (violet arrows) are defined as photons exiting the tissue in a central angle higher than 135 deg. Transmitted photons (blue arrows) are defined as photons exiting from the tissue on the opposite side of the tissue in a central angle lower than 45 deg.

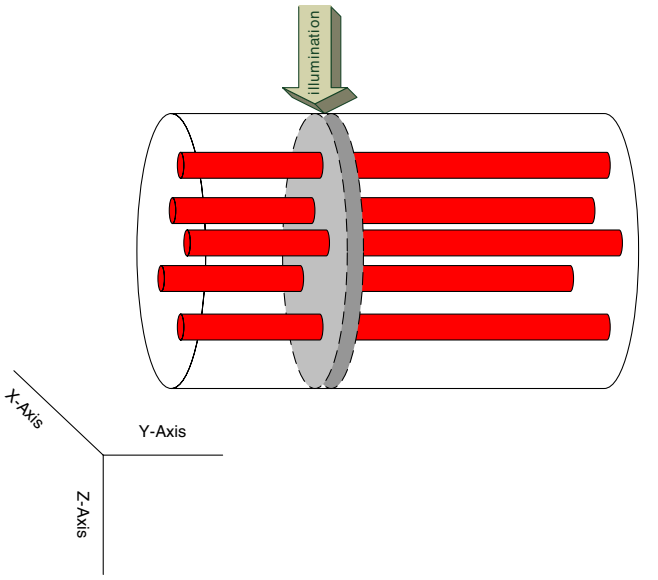

Fig. 2 The cross-section of simulated 3-D model of tissue with blood vessels.

highly scattering disturbances[9] in a tissue which is mainly a scattering medium.[23] The propagation path of each photon is calculated from the absorption and scattering constants (Table 1). An MC simulation of photon migration within irradiated tissues was performed based on the model that was previously developed in our group.[1] This simulation is based on the assumption that all photons reaching the tissue begin as ballistic photons (phase function equal to 0). Given the current photon's direction (θ_{old}), the new photon direction (θ_{new}) following tissue or blood vessels penetration was calculated according to the scattering and absorption properties, as follows:

1. The probability of a photon to survive was determined by $\exp(-\mu_a dr)$.
2. The probability of a photon to scatter was hence $[1-\exp(-\mu_s dr)]$. If the photon scattered, its new direction was calculated according to the following equation:

$$\theta_{\text{new}} = \theta_{\text{old}} + s \times \cos(g),$$

where s is a random number from the group $\{-1, 1\}$.

3. The dr steps were 80 μm while $dr \ll$ tissue diameters (D_t—see Table 2) and $dr < D$.

This process is repeated until the photon exits the tissue, and then its location is saved.

Ten repetitions of the simulation, where the number of vessels and their diameter were the same but their location was changed, were held to determine the variations due to the random blood vessel locations.

3 Results and Discussion

The simulation described in Sec. 2 was held for several vessel diameters while maintaining a constant blood volume. The mean fraction of photons that exited the tissue at several central angles (θ in Fig. 1) from 0 deg to 180 deg is presented in Fig. 3 for each vessel diameter. The mean of 10 different vessel

Table 1 Tissue and vessel optical properties for a wavelength of 850 nm.

Quantity	Symbol	Value	Units
Tissue absorption coefficient	$\mu_{a,t}$	0	cm^{-1}
Tissue scattering coefficient	$\mu_{s,t}$	10	cm^{-1}
Vessel absorption coefficient	$\mu_{a,v}$	0.415	cm^{-1}
Vessel scattering coefficient	$\mu_{s,v}$	780	cm^{-1}
Blood concentration	K	0.05	Dimensionless
Tissue anisotropy of scattering	g_t	0.8	Dimensionless
Vessel anisotropy of scattering	g_v	0.95	Dimensionless
Blood vessel diameters	D	2236, 1000, 710, 502, 355, 224.5, 159	μm
Number of blood vessels	n	1, 5, 10, 20, 40, 100, 200	Dimensionless

distributions was calculated. As can be seen from Fig. 3, for central angles lower than 135 deg the photon transmission decreases for lower vessel diameters, while for central angles higher than 135 deg the photon reflection decreases for higher vessel diameters. Thus, $\theta = 135$ deg is an isobaric point to vessel diameter.

In order to facilitate the presentation, reflected photons are defined as those that exit the tissue near the entrance point at a central angle of $|\theta| > 135$ deg. Forward transmitted photons are defined as those that exit the tissue at a central angle of $|\theta| < 45$ deg. Figure 4(a) and 4(b) presents the average fractions of the reflected and forward transmitted photons, respectively, for several vessel diameters while maintaining a constant blood volume. The standard deviation (STD) due to vessel placement is presented in both figures. These results match the "shielding effect"[10] since for larger blood vessels the total effective absorption and scattering are lower. As a result, the attenuation n is lower, hence the transmission is higher and the reflectance is lower as seen in Fig. 4(a) and 4(b). Note that the transmission curve in Fig. 4(b) matches the results presented by Jacques[13] for reflection. The changes in the scattering values near 850 nm wavelength are negligible and the changes in the absorption are still dominant.[3] It follows that less absorption will lead to more transmission and less reflectance as demonstrated.

Due to the fact that real tissues are 3-D and not 2-D, the 3-D simulation described in Sec. 2 was held, and the fraction of the reflection as a function of blood vessel diameter was presented [Fig. 4(c)], while keeping a constant blood volume. Despite the differences in the slopes and the variables, the 3-D curves resemble those received in the 2-D simulation.

Table 2 Comparison of average reflection (R_{avg}) and transmission (T_{avg}) for different tissue diameters (D_t).

D_t (mm)	R_{avg}	T_{avg}
5	0.0022 ± 0.0005	0.6893 ± 0.0309
10	0.4228 ± 0.0055	0.1518 ± 0.0030
15	0.0351 ± 0.0054	0.3965 ± 0.0476

However, the exact position of the isobaric point as well as the profile of transmitted photons strongly depends on the optical properties as well as the geometry of the tissue. As seen in Table 2, even if only the D_t changes while the number of vessels (n) is kept constant, the behavior of the transmitted and reflected photons switches and the isobaric point moves to a higher angle (~160 deg) for $D_t = 15$ mm and to a lower angle (~30 deg) for $D_t = 5$ mm.

The main result in the 2-D simulation is that for a central angle lower than the isobaric point the photon transmission is lower for vessels of lower diameter while for a central angle higher than the isobaric point the photon reflection is smaller for vessels of higher diameter. The latter result is in contrast to that obtained by Jacques,[13] who used a semi-infinite model of the tissue and a wavelength of 585 nm. While repeating Jacques' conditions we were able to reproduce his results. This outcome

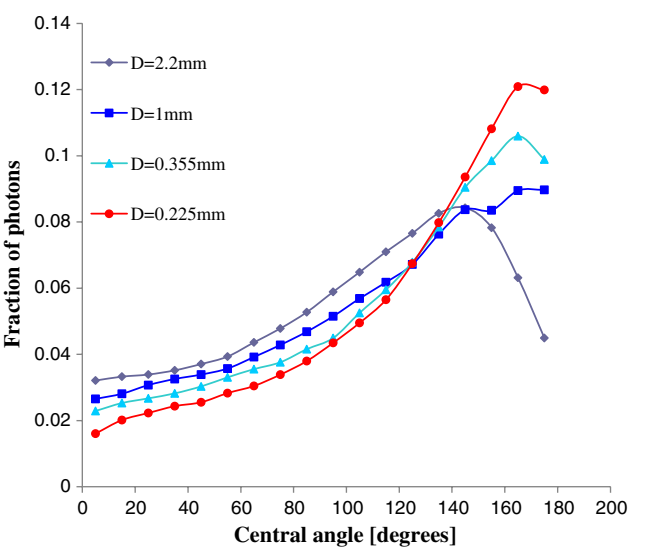

Fig. 3 The distribution of collected photons. The percent of photons exiting from the tissue in different central angles for various vessel diameters. For central angles lower than 135 deg the photon transmission increases for higher vessel diameters; for central angles higher than 135 deg the photon reflection decreases for higher vessel diameters.

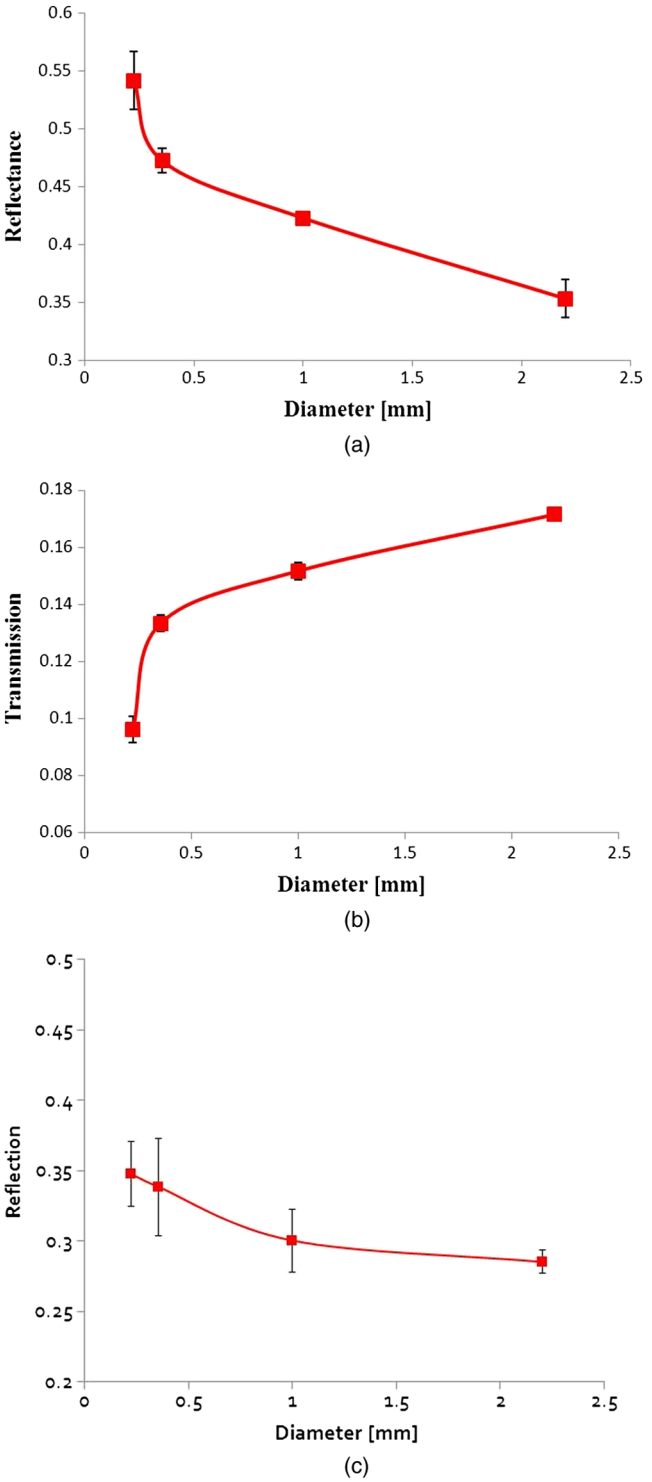

Fig. 4 The fraction of (a and c) reflected and (b) forward transmitted photons as a function of blood vessel diameter while keeping a constant blood volume, obtained by computerized simulation for (a and b) 2-D and (c) 3-D.

reinforces the correctness of our model. The reasons that we found that the photon reflection is smaller for vessels of higher diameter are the difference in: (1) the wavelengths (585 nm at Jacques and 850 nm in this research); and following this (2) the absorption constant (168 cm^{-1} at Jacques) is 36 times higher than the absorption constant for the wavelength chosen in our paper[21] which has a value of 4.67 cm^{-1}. Furthermore, (3) an 850 nm wavelength provides higher penetration depth and (4) lower tissue scattering.[3] However, both the scattering profile as well as the value of the isobaric point strongly depend on optical properties (like the absorption and scattering constants) and the exact geometry of the case (as we shown for different D_t).

4 Conclusion

The main result is that there is a central angle that below which the photon transmission decreased for lower vessel diameters while above this angle the opposite occurred. The isobaric point (found at $\theta = 135$ deg under the presented studies conditions) could be used as a point of measurement for optical characterization purposes. Furthermore, the findings of our work dealing with the changes in reflection and transmission for different blood vessels diameter with the same volume could be used for different applications such as pulse oximetry in the ear lobe as well as in pinched tissue or in the fingertip joint. The changes in the scattering profile due to variations in blood vessel diameter are more substantial than the change in optical properties in the NIR region, and hence may be used to improve existing pulse oximetry methods. The current pulse oximetry technique derives oxygen saturation in arterial blood from light transmission pulses (photoplethysmography) signals in two wavelengths. The current technique requires calibration and the calibration process saves the need for separation between absorption and scattering effects, and also the need for exact knowledge of the light extinction coefficients. By using our new computer simulation for the evaluation of the transmission and reflection of NIR photons after being scattered and absorbed, the accurate values of extinction coefficients can be extracted and will improve the pulse oximetry technique as well as other NIR methods for the assessment of oxygen saturation.

References

1. R. Ankri et al., "In-vivo tumor detection using diffusion reflection measurements of targeted gold nanorods—a quantitative study," *J. Biophoton.* **5**(3), 263–273 (2012).
2. R. Ankri, H. Taitelbaum, and D. Fixler, "Reflected light intensity profile of two-layer tissues: phantom experiments," *J. Biomed. Opt.* **16**(8), 0850011–0850016 (2011).
3. D. Fixler and R. Ankri, "Subcutaneous gold nanorod detection with diffusion reflection measurement," *J. Biomed. Opt.* **18**(6), 612261–612267 (2013).
4. R. A. J. Groenhuis, A. H. Ferweda, and J. J. Ten Bosch, "Scattering and absorption of turbid materials determined from reflection measurements. 1: theory," *Appl. Opt.* **22**(16), 2456–2462 (1983).
5. D. Jakubowski et al., "Quantitative absorption and scattering spectra in thick tissues using broadband diffuse optical spectroscopy," Chapter 12 in *Biomedical Optical Imaging*, J. G. Fujimoto and D. L. Farkas, Eds., pp. 330–355, Oxford University Press, New York (2009).
6. T. H. Pham et al., "Broad bandwidth frequency domain instrument for quantitative tissue optical spectroscopy," *Rev. Sci. Instrum.* **71**(6), 2500–2513 (2000).
7. M. Friebel et al., "Influence of oxygen saturation on the optical scattering properties of human red blood cells in the spectral range 250 to 2000 nm," *J. Biomed. Opt.* **14**(3), 034001–034006 (2009).
8. M. Friebel et al., "Determination of optical properties of human blood in the spectral range 250 to 1100 nm using Monte Carlo simulations with hematocrit-dependent effective scattering phase functions," *J. Biomed. Opt.* **11**(3), 034021 (2006).
9. A. Roggan et al., "Optical properties of circulating human blood in the wavelength range 400–2500 nm," *J. Biomed. Opt.* **4**(1), 36–46 (1999).
10. L. Zhang, A. Shi, and H. Lu, "Determination of optical coefficients of biological tissue from a single integrating-sphere," *J. Mod. Opt.* **59**(2), 121–125 (2012).

11. R. Vered, S. Havlin, and H. Taitelbaum, "Optical detection of hidden tumors," *Proc. SPIE* **2389**, 851–858 (1995).
12. M. Firbank, E. Okada, and D. T. Delpy, "Investigation of the effect of discrete absorbers upon the measurement of blood volume with near-infrared spectroscopy," *Phys. Med. Biol.* **42**(3), 465–477 (1997).
13. S. L. Jacques, "Optical assessment of cutaneous blood volume depends on the vessel size distribution: a computer simulation study," *J. Biophoton.* **3**(1–2), 75–81 (2010).
14. H. Liu et al., "Influence of blood vessels on the measurement of hemoglobin oxygenation as determined by time-resolved reflectance spectroscopy," *Med. Phys.* **22**(8), 1209–1217 (1995).
15. A. Talsma, B. Chance, and R. Graaff, "Corrections for inhomogeneities in biological tissue caused by blood vessels," *J. Opt. Soc. Am.* **18**(4), 932–939 (2001)
16. A. N. Yaroslavsky et al., *Optics of Blood*, SPIE Press, Bellingham (2002).
17. G. Zaccanti, S. Del Bianco, and F. Martelli, "Measurements of optical properties of high-density media," *Appl. Opt.* **42**(19), 4023–4030 (2003)
18. S. L. Jacques and B. W. Pogue, "Tutorial on diffuse light transport," *J. Biomed. Opt.* **13**(4), 041302 (2008).
19. L. Wang and S. L. Jacques, "Hybrid model of Monte Carlo simulation and diffusion theory for light reflectance by turbid media," *J. Opt. Soc. Am. A* **10**(8), 1746–1752 (1993).
20. L. Wang, S. L. Jacques, and L. Zheng, "MCML—Monte Carlo modeling of light transport in multi-layered tissues," *Comput. Methods Prog. Biomed.* **47**(2), 131–146 (1995).
21. M. Nitzan and S. Engelberg, "Three-wavelength technique for the measurement of oxygen saturation in arterial blood and in venous blood," *J. Biomed. Opt.* **14**(2), 024046-1–024046-6 (2009).
22. X. Guo et al., "Depolarization of light in turbid media: a scattering event resolved Monte Carlo study," *Appl. Opt.* **49**, 153–162 (2010).
23. A. N. Bashkatov et al., "Optical properties of human skin, subcutaneous and mucous tissues in the wavelength range from 400 to 2000 nm," *J. Phys. D: Appl. Phys.* **38**(15), 2543–2555 (2005).